

# An angle-independent Frequency Selective Surface in the optical range

Daniel Van Labeke, Davy Gérard, Brahim Guizal and Fadi I. Baida

Institut FEMTO-ST, UMR CNRS 6174, Université de Franche-Comté, Route de Gray,  
25030 Besançon cedex, France

[fbaida@univ-fcomte.fr](mailto:fbaida@univ-fcomte.fr)

Lifeng Li

State Key Laboratory of Precision Measurement Technology and Instruments, Department of  
Precision Instruments, Tsinghua University, Beijing 100084, People's Republic of China

**Abstract:** We suggest and numerically demonstrate a design for Frequency Selective Surfaces (FSS) operating in the optical (visible and near-infrared) range. The position and width of the FSS bandpass do not depend on the angle of incidence and polarization state of the incoming light, allowing high transmission at any angle. The FSS is formed by annular apertures perforated in a metal film and arranged in a square array. Angle- and polarization-independent transmission properties are demonstrated for silver. These results can be extended to other metals as well as to other frequency domains.

© 2006 Optical Society of America

**OCIS codes:** (050.1220) Diffraction and gratings: Apertures ; (230.7370) Optical devices: Waveguides ; (240.6680) Optics at surfaces: Surface plasmons

---

## References and links

1. B.A. Munk, *Frequency Selective Surfaces: Theory and Design*, John Wiley and sons, New York, 2000
2. S.J. Spector, D.K. Astolfi, S.P. Doran, T.M. Lyszczarz and J.E. Raynolds, "Infrared frequency selective surfaces fabricated using optical lithography and phase-shift masks," *J. Vac. Sci. Technol. B* **19**, 2757-2760 (2001)
3. A. Sentenac and A.-L. Fehrembach, "Angular tolerant resonant grating filters under oblique incidence," *J. Opt. Soc. Am. A* **22**, 475-480 (2005)
4. T.W. Ebbesen, H. J. Lezec, H. F. Ghaemi, T. Thio, and P. A. Wolff, "Extraordinary optical transmission through sub-wavelength holes arrays," *Nature (London)* **391**, 667-669 (1998)
5. E. Popov, S. Enoch, G. Tayeb, M. Nevière, B. Gralak and N. Bonod, "Enhanced transmission due to nonplasmon resonances in one-and two-dimensional gratings," *Appl. Opt.* **43**, 999-1008 (2004)
6. A. Roberts and R. MacPhedran, "Bandpass Grids with Annular Apertures," *IEEE Trans. Antennas. Propag.* **36**, 607-611 (1988).
7. T. K. Wu, "Infrared filters for high-efficiency thermovoltaic devices," *Microwave and optical technology letters*, **15**, 9-12 (1997).
8. F.I. Baida and D. Van Labeke, "Light transmission by subwavelength annular aperture arrays in metallic films," *Opt. Commun.* **209**, 17-22 (2002)
9. A. Moreau, G. Granet, F. Baida, and D. Van Labeke, "Light transmission by subwavelength square coaxial aperture arrays in metallic films," *Opt. Express* **11**, 1131-1136 (2003) <http://www.opticsinfobase.org/abstract.cfm?URI=oe-11-10-1131>
10. M. G. Moharam and T. K. Gaylord, "Rigorous coupled-wave analysis of metallic surface-relief gratings," *J. Opt. Soc. Am. A* **3**, 1780-1787 (1986)
11. G. Granet and J.-P. Plumey, "Parametric formulation of the Fourier modal method for crossed surface-relief gratings," *J. Opt. A: Pure. Appl. Opt* **4**, 145-149 (2002)
12. B. Bai and L. Li, "Group-theoretic approach to enhancing the Fourier modal method for crossed gratings with square symmetry," *J. Opt. Soc. Am. A* **23**, 572-580 (2006)

13. The wavelength dependence of the dielectric constant of silver is described by a Drude model:  $\epsilon = 1 - \omega_p^2 / (\omega(\omega + i\gamma))$ , where  $\omega_p = 1.374 \times 10^{16} \text{ rad.s}^{-1}$  and  $\gamma = 3.21 \times 10^{13} \text{ rad.s}^{-1}$ .
14. W. Fan, S. Zhang, B. Minhas, K.J. Malloy, and S.R.J. Bruek, "Enhanced Infrared Transmission through Sub-wavelength Coaxial Metallic Arrays," *Phys. Rev. Lett.* **94**, 033902 (2005)
15. J. Salvi, M. Roussey, F. I. Baida, M.-P. Bernal, A. Mussot, T. Sylvestre, H. Maillotte, D. Van Labeke, A. Perentes, I. Utke, C. Sandu, P. Hoffmann and B. Dwir, "Annular aperture arrays: study in the visible region of the electromagnetic spectrum," *Opt. Lett.* **30**, 1611 (2005)
16. F.I. Baida, D. Van Labeke, G. Granet, A. Moreau and A. Belkhir, "Origin of the super-enhanced light transmission through a 2-D metallic annular aperture array: a study of photonic bands," *Appl. Phys. B* **79**, 1-8 (2004)
17. E. Popov, M. Nevière, S. Enoch and R. Reinisch, "Theory of light transmission through subwavelength periodic hole arrays," *Phys. Rev. B* **62**, 16100-16108 (2000)
18. Ph. Lalanne, J.C. Rodier and J.P. Hugonin, "Surface plasmons of metallic surfaces perforated by nanohole arrays," *J. Opt. A: Pure Appl. Opt.* **7** 422-426 (2005)
19. Z. Ruan and M. Qiu, "Enhanced transmission through periodic arrays of subwavelength holes: the role of localized waveguide resonances," *Phys. Rev. Lett.* **96**, 233901 (2006)
20. Q. Cao and Ph. Lalanne, "Negative Role of Surface Plasmons in the Transmission of Metallic Gratings with Very Narrow Slits," *Phys. Rev. Lett.* **88**, 057403 (2002)
21. F. Marquier, J. Greffet, S. Collin, F. Pardo, and J. Pelouard, "Resonant transmission through a metallic film due to coupled modes," *Opt. Express* **13**, 70-76 (2005) <http://www.opticsinfobase.org/abstract.cfm?URI=oe-13-1-70>
22. J.T. Shen, P.B. Catrysse and S. Fan, "Mechanism for Designing Metallic Metamaterials with a High Index of Refraction," *Phys. Rev. Lett.* **94**, 197401 (2005)

Frequency Selective Surfaces (FSS) are metallic grids that are able to transmit or reflect the electromagnetic radiation with frequency discrimination. FSS are well-known and widely used in the microwave domain, for instance as reflectors in antenna applications, as an electromagnetic window or for screening a radar emitter/transmitter from hostile emissions [1]. More recently, FSS were designed in the mid-infrared range [2]. In principle, an ideal FSS should exhibit a passband or stopband of constant width and spectral position with respect to angle of incidence and polarization of the waves impinging on it. However, such a property is difficult to obtain and most FSS operate around a fixed angle of incidence. One common solution is to use a multi-layered FSS (each layer presenting different geometrical parameters) but this leads to oversized structures and may increase the losses.

At optical frequencies, realization of compact angle-independent filters is a challenging task. Interference filters (Bragg mirrors), which are one of the most common optical components, are angle sensitive and must be used at or near normal incidence. In order to obtain narrow-band filters with a larger angular tolerance, it is possible to use a multilayer stack or a resonant structure [3], but the resulting angular window remains small. Metallic films perforated with arrays of sub-wavelength apertures [4] were once thought to be promising candidates for compact filtering. Unfortunately, the transmission properties of these structures rely partly on a coupling with surface electromagnetic waves (surface plasmons) whose optical properties critically depend on the angle of incidence. As a consequence, the bandpass position shifts with the angle of incidence.

In this paper, we propose a new FSS design allowing angle- and polarization-independent transmission in the optical (visible and near-infrared) domain. It is an array of sub-wavelength annular apertures perforated on a metal film. In contrast to Ref. [4], the high transmission and the general shape of the spectra (Fabry-Pérot like spectra) do not rely on surface modes, but rather on a cavity mode whose resonant frequency is angle-independent. However, in the vicinity of an anomaly, a coupling between a surface mode and the cavity mode occurs and the Fabry-Pérot spectrum is perturbed: the surface plasmon destroys the high transmission. We numerically demonstrate that for a well-chosen metal thickness, angle-independent transmission bands are obtained. The absolute transmission in the band is more than 80%. The tolerance on polarization is also excellent. The interesting properties of our structure are caused by the occurrence of a cavity resonance. Recently Popov *et al.* [5] have presented interesting results, in

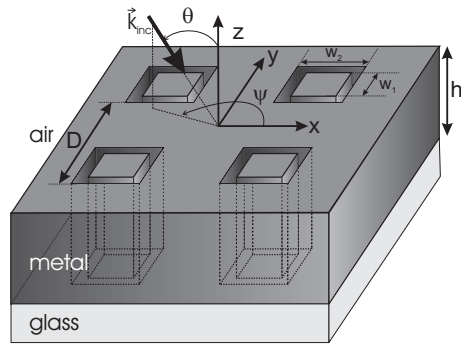


Fig. 1. Sketch of the structure.

the far-infrared or microwave domains, of high transmission due to nonplasmon resonances for one and two-dimensional gratings (Fabry-Pérot, waveguide or cavity resonances) It is important to underline that in the microwave region A. Roberts et al. Have theoretically established the band-pass property of a metallic grid with circular apertures. [6]. More recently T.K. Wu [7] has described the filtering properties of thin FSS grids, designed for applications in the infrared, with circular or square loops patterns. He stated that the performances of those filters are stable despite variations in the illumination angle and polarization. In our paper, we establish that these interesting properties of the 2D array of coaxial cavities remain valid in the visible region despite the losses of the metals (Silver or Gold) in this spectral region.

The design of the FSS is schematically represented in Fig. 1. It is based on the Annular Aperture Array (AAA): a square array of square annular apertures is patterned on a metal film deposited on a glass substrate (optical index  $n_3$ ). The period of the grating is  $D$ , the inner and outer widths of the apertures are  $w_1$  and  $w_2$ , respectively. The metal thickness is  $h$  and its optical properties are described by a dispersive complex dielectric constant.

A plane wave impinges from the air side of the structure with angle of incidence  $\theta$ . The orientation of the plane of incidence is located by the azimuthal angle  $\psi$  measured from the  $x$ -axis. The theoretical study of the diffracted intensities remains a difficult problem. In the past, various methods have been developed to obtain spectral responses of AAA structures. Roberts *et al.* used a modal method [6]. The recent studies in the visible region [8] were performed with a FDTD algorithm, a powerful but memory- and time-consuming method. These FDTD results were strengthened [9] by computations using the Fourier Modal Method (FMM) also known in the literature as the Rigorous Coupled Wave Method [10]. In this letter modeling has been performed using a highly-improved FMM algorithm [11, 12]. Compared to the previous method, our FMM algorithm presents two major improvements. First, it uses an appropriate coordinate system in order to take into account sharp edges [11]. Second, it fully exploits the symmetries of the structure: this leads to a strong reduction of both computation time and required memory [12]. It is worth noticing that the FMM algorithm is more efficient for rectangular apertures than for circular ones: this is why we focus on square apertures. However, we emphasize that the transmission properties of the AAA structure do not depend much on the shape of the apertures (square apertures or ring apertures) [8, 9].

The transmission properties of the AAA structure as a function of the metal thickness are reported in Fig. 2. The structure parameters are  $D = 300\text{nm}$ ,  $w_1 = 105\text{nm}$  and  $w_2 = 150\text{nm}$ . The incident medium is air ( $n_1 = 1$ ), the metal is silver [13] and the substrate is glass ( $n_3 = 1.5$ ). A structure with such submicronic parameters can be fabricated by interferometric lithography

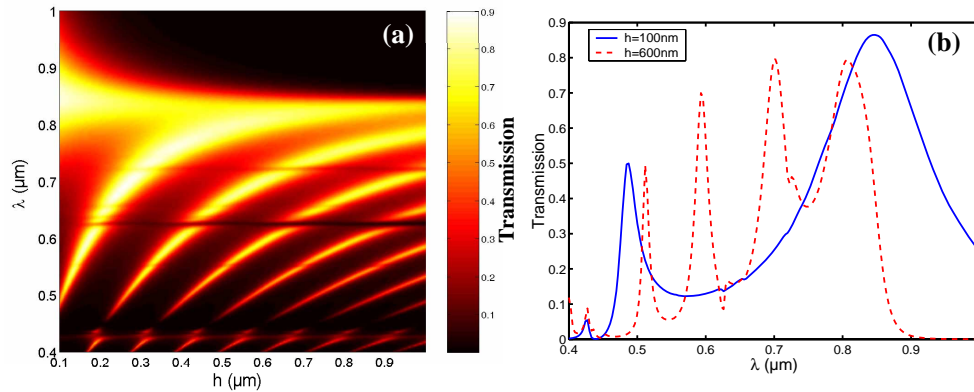


Fig. 2. Calculated transmission through the FSS for normal incidence. (a) Evolution of the transmission efficiency (color scale) as a function of the metal film thickness and incident wavelength. (b) Cross section of Fig. 2(a) for two different thicknesses,  $h=100\text{nm}$  (solid line) and  $h=600\text{nm}$  (dashed line).

[14] or by milling with a focused ion beam [15]. A  $p$ -polarized (TM) monochromatic electromagnetic plane wave (electric field in the plane of incidence) illuminates the structure. Its wave vector is kept in the  $(x, z)$  plane (i.e.  $\psi = 0$ ) and forms an angle  $\theta$  with the  $z$ -axis. In Fig. 2(b) are shown the transmission spectra for two metal thicknesses (100nm and 600nm). In both cases, the transmission spectrum exhibits broad and well-defined resonances in the optical region and a very large efficiency ( $T > 80\%$ ) at the resonant wavelength. Only two peaks appear for  $h = 100\text{nm}$  whereas four peaks have a significant intensity for  $h = 600\text{nm}$ . Transmission spectra of AAA structures have been interpreted in previous papers [16], but let us recall briefly the underlying physical process. In metallic films perforated with sub-wavelength cylindrical apertures [4], the holes do not support any propagative mode. The observed enhanced transmission is generally explained by a coupling between surface plasmons propagating along the horizontal metal surface and the aperture's evanescent vertical modes. The transmission remains rather small (less than 20%), due to the role of this evanescent modes. In the case of the AAA structure, the enhanced transmission does not stem from surface plasmon resonances or Rayleigh anomalies. It arises from the resonant excitation of *one* cavity mode which propagates in the coaxial aperture. This mode is a  $\text{TE}_{11}$ -like mode which is a propagative mode with a small attenuation. Compared to the cylindrical waveguide, the coaxial waveguide (with the same external radius or width) supports a mode with a larger cutoff wavelength. In the studied case ( $w_1 = 105\text{nm}$ ,  $w_2 = 150\text{nm}$  and silver) the cutoff of the  $\text{TE}_{11}$ -like mode is around  $\lambda = 900\text{nm}$ , leading to a propagative mode for all the visible spectrum. In spite of the small lateral dimensions of the air gap, the coaxial cavity acts as a Fabry-Pérot resonator. As a consequence, the spectral position of the resonant mode does not depend on the periodicity. However, we stress that the periodic structure plays an important role: it acts as a grating coupler allowing the incident plane waves to efficiently excite the guided mode and reciprocally, coupling the guided mode to plane waves on the exit side. This behavior bears some resemblance with the properties of lamellar gratings (metallic films perforated with an array of slits). A single slit also exhibits a propagative guided mode regardless of its width, the TEM mode which has no cutoff frequency [17]. Nevertheless, there are two crucial differences between the AAA structure and the lamellar grating. First, the TEM mode of the lamellar grating requires a minimum metal thickness to exist, whilst this is not the case for the  $\text{TE}_{11}$  mode in the coaxial waveguide (cf. Fig 2(b), solid

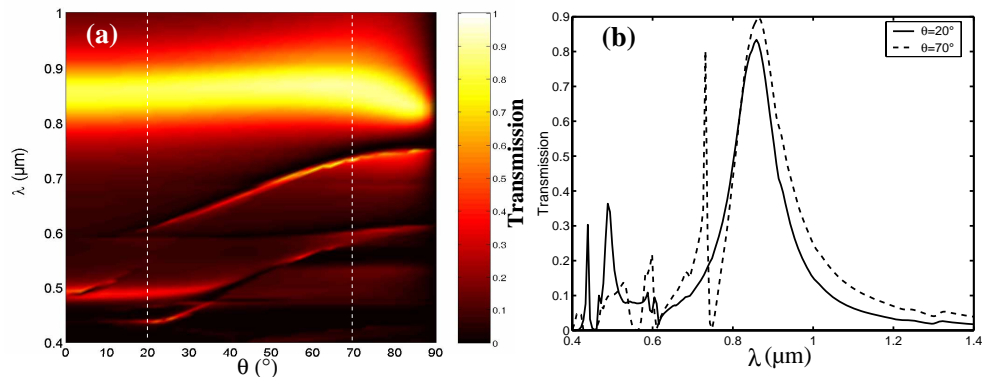


Fig. 3. Calculated transmission through the FSS for  $h = 100\text{nm}$ . (a) Evolution of the transmission efficiency (color scale) as a function of the angle of incidence and incident wavelength. (b) Cross section of (a) along the two vertical dashed lines.

line). Second, the TEM mode is excited only for an incident electric field perpendicular to the slits. This strong polarization dependence makes the lamellar grating a poor candidate for the FSS applications we are looking for.

Fig. 2(a) shows the transmission efficiency (color scale) as a function of the metal thickness and the illumination wavelength, for normal incidence. It is clear from this figure that there is a resonance which wavelength position does not depend on the metal thickness (horizontal band near  $\lambda = 860\text{nm}$ ). This resonance corresponds to the  $\text{TE}_{11}$ -like mode excited at its cutoff wavelength. The other resonances asymptotically converge towards the cutoff wavelength. They correspond to harmonics of the  $\text{TE}_{11}$ -like mode. The excitation of a guided mode at its cutoff frequency may appear quite surprising, since to the best of our knowledge it is not discussed in classical textbooks. To explain this feature, we describe the transmission spectra by a simple phenomenological model which corresponds to the excitation of only one mode in the cavity [18]:

$$t = \frac{t_1 t_2 e^{ik_z h}}{1 + r_1 r_2 e^{2ik_z h}}, \quad (1)$$

where  $t$  is the complex transmission coefficient. This equation is very similar to the equation describing the transmission through a slab or a Fabry-Pérot resonator,  $t_1$  and  $t_2$  playing the role of the transmission coefficients of the two interfaces,  $r_1$  and  $r_2$  being the corresponding reflection coefficients. The factor  $e^{ik_z h}$  corresponds to the propagation in the cavity. By introducing in (1) the dispersion relation of the  $\text{TE}_{11}$  mode with a cutoff frequency  $\omega_c$  ( $k_z \simeq \sqrt{(\omega^2 - \omega_c^2)}/c$ ) it is possible to reproduce quite fairly the behavior observed in Fig. 2. At the cutoff frequency  $k_z$  equals zero, leading to a resonance for all metal thicknesses. This point was also discussed in a very recent paper by Ruan and Qiu [19]: for a metallic film with a periodic array of rectangular holes a high transmission could also be obtained by exciting a guided mode at its cutoff, leading also in this case to a transmission peak independent of metal thickness.

The behavior of the transmission spectra vs. the angle of incidence is given in Fig. 3(a), for  $h = 100\text{nm}$ . The striking result is that the resonant wavelength of the mode is almost angle-independent: for all angles between  $0$  and  $80^\circ$ , the resonant wavelength remains the same (horizontal band at  $\lambda \simeq 860\text{nm}$ ). Moreover, the cross sections of Fig. 3(b) (for  $\theta = 20^\circ$  and  $\theta = 70^\circ$ ) show that the resonance maximum and bandwidth do not change from one angle to

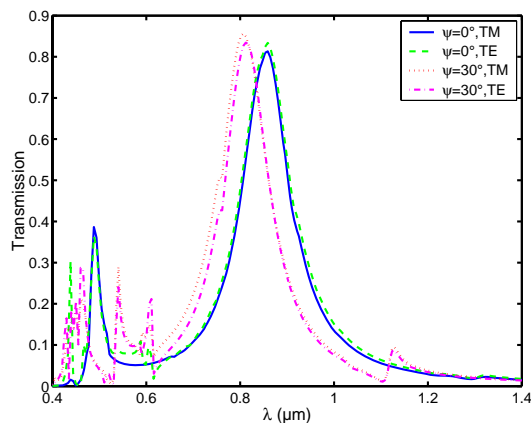


Fig. 4. Transmission spectra for  $\theta = 20^\circ$ : TM (solid line) and TE (dashed line) for an azimuthal angle  $\psi = 0^\circ$ ; TM (dotted line) and TE (dash-dotted line) for  $\psi = 30^\circ$ .

another. These properties are characteristic of a FSS. Transmission anomalies appear for wavelengths shorter than the fundamental waveguide resonance (dark lines in Fig. 3(a)). When one of these anomalies approaches a cavity resonance, the coupling between the two leads to a deterioration of the transmission efficiency. A similar behavior has been discussed for a lamellar grating [20, 21]. This also explains why the transmission band at  $\lambda \simeq 860\text{nm}$  is disturbed for angles larger than  $\theta = 80^\circ$ . For future applications, it would be necessary to adjust the geometrical parameters of the structure to avoid such a collision. Let us emphasize that these anomalies disappear in the case of TE polarization, suggesting that they might be linked to surface plasmon resonances. Note that anomalies also appear in Fig. 2(a) as horizontal dark lines. The line near  $\lambda = 450\text{nm}$  is probably linked to a Rayleigh-Wood anomaly. The anomalies appearing at higher wavelengths are more difficult to analyze. They also appear on spectra calculated with a FDTD algorithm, confirming that they are not numerical artifacts. We believe that localized resonances (such as localized plasmons excited in the aperture corners) may explain these anomalies. Further investigations are in progress.

In order to get an ideal FSS there is one more condition to fulfill: the transmission properties must be independent on the polarization and the azimuthal angle  $\psi$  of the incoming wave. Under normal incidence, simple symmetry considerations show that TE and TM polarizations are equivalent, but this is no longer true for  $\theta \neq 0$  or  $\psi \neq 0$ . The evolution of the transmission spectra with the polarization is reported in Fig. 4. For an arbitrary angle of incidence ( $\theta = 20^\circ$ ), the figure shows the transmission spectra for the TE and TM polarization states for two tilt angles:  $\psi = 0^\circ$  (solid and dashed lines) and  $\psi = 30^\circ$  (dotted and dashed dotted lines). For a given azimuth  $\psi$ , the main resonant peak is independent on the polarization state. However, the peak slightly blue-shifts when one increases the azimuthal angle. This dependence vs. the azimuth could be drastically reduced by using circular apertures rather than square ones.

Other calculations (not shown here) demonstrate that the FSS effect is maintained for a perfectly conducting metal. This suggests that the same design could be used at higher wavelengths (microwave, THz, radio frequencies).

In conclusion, we have designed a Frequency Selective Surface operating in the optical range. The design is based on an annular aperture array that exhibits angle- and polarization-independent transmission properties. The transmission efficiency is very high, regardless of the state of polarization or the angle of incidence of the incoming wave. Furthermore, the

same design can be applied to other metals (e.g. gold or aluminium at visible and infrared frequencies) with similar performances. The extension to the microwave or THz region of the spectrum (where most metals are almost perfectly conducting) is straightforward and has been checked. This finding may evoke numerous applications in optics and electromagnetics, for instance in the design of compact filters for integrated semiconductor lasers (VCSELs), electromagnetic windows at telecom wavelengths or, in the microwave domain, for radome applications. The AAA structure leads to bandpass filters but with very wide widths. However there are applications where a broad bandwidth is sufficient. If necessary, it is possible to reduce the bandwidth by using superimposed structures [5]. From a more fundamental point of view, the complex interplay between grating anomalies and guided modes needs further investigations. Another interesting perspective is suggested by the work of Shen *et al.* [22] who have considered a lamellar grating as a metamaterial exhibiting an effective index of refraction. It would certainly be enlightening to consider the AAA structure under the same point of view and to investigate what effective properties can be deduced from its angular and spectral behavior.

This work has been supported by the European Network of Excellence on Micro Optics (NEMO). The work of L. Li has been supported by the National Science Fund for Distinguished Young Scholars established by the National Natural Science Foundation of China under project 60125514.